Stratum corneum model membranes : molecular organization in relation to skin barrier function

Groen, D.

Chapter 2

Two new methods for preparing a unique stratum corneum substitute

Daniël Groen, Gert S. Gooris, Maria Ponec, Joke A. Bouwstra

Biochim Biophys Acta, vol. 1778, no. 10, pp. 2421-2429.

Abstract

Stratum corneum lipids play an important role in the barrier function of skin. An in vitro permeation model consisting of synthetic lipids has previously been developed to replace human stratum corneum (SC) in permeation studies. This model is referred to as the stratum corneum substitute (SCS). In order to improve its reproducibility and to increase the efficiency in preparing the SCS, two new preparation methods are developed. Subsequently the properties of the SCS prepared by the various methods, i.e. the manual airbrush method, the rotor airbrush method and the linomat method, are investigated. The results show that the SCS prepared with the various methods share the properties of a uniform lipid composition and lipid distribution. Furthermore, irrespective of the preparation method, the lipids form crystalline lamellar phases, mimicking the lipid organization and orientation in human SC. As a result, permeation profiles of benzoic acid through SCS are very similar to human SC. The rotor method increases the efficiency and reproducibility of the manual airbrush method, while the linomat method reduces the lipid loss during preparation and results in SCS with a more uniform membrane thickness. In conclusion, the linomat method was chosen as the preferred method for preparing the substitute.

1. Introduction

The uppermost layer of the human skin, the stratum corneum (SC) consists of flattened dead skin cells (corneocytes) surrounded by lipid lamellae. The lipid domains in the SC form the only continuous pathway through the SC and are suggested to act as the main barrier for diffusion of substances through the skin (1). The main lipid classes in SC are ceramides (CER), cholesterol (CHOL) and free fatty acids (FFA) (2-5). The lipids are arranged in two coexisting lamellar phases; a long periodicity phase (LPP) with a repeat distance of ~13 nm and a short periodicity phase (SPP) with a repeat distance of ~6 nm (6, 7). Furthermore, within the lamellae the lipids form mainly a crystalline lateral packing. The lipid organization and its orientation approximately parallel to the skin surface play an important role in the skin barrier function (8). A more detailed analysis of the lipid composition revealed that the FFA has lipid chain lengths of mainly 22 and 24 C atoms (9). In addition, there are nine subclasses of CER in human SC (5). The CER consist of either a sphingosine (S), phytosphingosine (P) or a 6-hydroxysphingosine (H) base, whereas the acyl chain is a nonhydroxy (N), α-hydroxy (A) or ω-hydroxy chain (10). The corresponding nonhydroxy and α-hydroxy CER are therefore denoted as CER NP, CER NS, CER NH, CER AP, CER AS and CER AH. The ω-hydroxy CER possess a longer chain length (mainly between C_{30} and C_{34}) and have a linoleic acid chemically bound to their ω-hydroxy group (indicated with EO). They are denoted as CER EOP, CER EOS and CER EOH.

As there is a great interest in the administration of drugs via the skin, there is a need for predictive in-vitro permeation models. Isolated human epidermis or SC can serve as an excellent in-vitro model but human skin is scarcely available and the inter-individual variability of human skin is substantial. Furthermore, with respect to diseased skin, for which many topical drugs are developed, it is virtually impossible to obtain skin for in-vitro diffusion studies. Animal skin as an alternative is not an optimal choice as it

has different permeation properties than human skin. In addition, after 2009 there will be an EU ban on the use of animal skin for the testing of cosmetic products.

Because of the crucial role of the lipids in the skin barrier function, in previous studies an in-vitro model based on SC lipids was developed, referred to as the stratum corneum substitute (SCS) (11, 12). The SCS consists of a porous substrate covered with a layer of synthetic SC lipids. These lipids mimic very closely the molecular organization and orientation of the SC lipid lamellae. An advantage of the SCS is that its composition can be easily modified which allows us to study the relationship between lipid composition, molecular organization and barrier function in just one model. With the SCS we also have the unique possibility to mimic the lipid composition and organization of dry or diseased skin.

In previous studies, the SCS was prepared by spraying a lipid solution onto a substrate with a modified airbrush method. This preparation method results in a SCS with excellent barrier properties similar to SC. However, the spraying process is labor intensive and a substantial part of the lipid solution is lost to the air. Therefore the preparation method of the SCS requires further optimization. In the present study a method is developed to scale up the production of SCS making it less labor intensive. In addition, an alternative preparation method is presented to minimize the loss of lipids to the air. In order to validate the various preparation methods, the qualities of SCS prepared with the various methods are compared. The SCS are characterized concerning their 1) lipid composition and distribution, 2) thickness and profile of the lipid layer, 3) lipid loss during spraying, 4) lipid packing, 5) lamellar organization and orientation and 6) variation in equilibration temperature and permeation properties.

2. Materials and Methods

2.1 Materials

Synthetic CER(EOS)C30-linoleate, CER(NS)C24, CER(NP)C24, CER(NP)C16, CER(AS)C24 and CER(AP)C24 were generously provided by Cosmoferm B.V. (Delft, The Netherlands). Palmitic acid (C16:0), stearic acid (C18:0), arachidic acid (C20:0), behenic acid (C22:0), tricosanoic acid (C23:0), lignoceric acid (C24:0), cerotic acid (C26:0) and cholesterol were purchased from Sigma-Aldrich Chemie GmbH (Schnelldorf, Germany). Perdeuterated palmitic and behenic acid were purchased from Larodan (Malmö, Sweden), perdeuterated stearic and arachidic acid from Cambridge Isotope Laboratories (Andover, Massachusetts) and perdeuterated lignoceric acid was purchased from Arc Laboratories B.V. (Apeldoorn, The Netherlands). Benzoic acid, trypsin (type III, from bovine pancreas), and trypsin inhibitor (type II-S from soybean) were obtained from Sigma-Aldrich (Zwijndrecht, The Netherlands). Dialysis membrane disks (cutoff value of 5000 Da) were obtained from Diachema (Munich, Germany). Nuclepore polycarbonate filter disks (pore size 50 nm) were purchased from Whatman (Kent, UK). All organic solvents are of analytical grade and manufactured by Labscan Ltd. (Dublin, Ireland). All other chemicals are of analytical grade and the water is of Millipore quality.

2.2 Isolation of SC from human skin

SC was isolated from abdominal or mammary skin, which was obtained within 24 h after cosmetic surgery. After removal of the subcutaneous fat tissue, the skin was dermatomed to a thickness of approximately 250 μm using a Padgett Electro Dermatome Model B (Kansas City, KS, USA). The SC was separated from the epidermis by trypsin digestion [0.1% in phosphate-buffered saline (PBS), pH 7.4], after overnight incubation at 4ºC and subsequently at 37ºC for 1 h. The SC was then placed in a 0.1% solution of trypsin inhibitor and rinsed twice with Millipore water.

Until use, the SC was stored in a silica-containing box under gaseous nitrogen or argon in the dark to prevent oxidation of the intercellular SC lipids.

2.3 Preparation of the SCS

2.3.1 Preparing the lipid mixture

For the preparation of the SCS, CHOL, synthetic CER and FFA were used. The following synthCER composition was selected: CER(EOS)C30, CER(NS)C24, CER(NP)C24, CER(AS)C24, CER(NP)C16 and CER(AP)C24 in a 15:51:16:4:9:5 molar ratio which closely resembles the CER composition in pig SC (13). This synthCER composition is similar to that used in our previous studies (12, 14). The acyl chain length is either 30 C atoms (C30), 24 C atoms (C24) or 16 C atoms (C16). For the free fatty acids mixture (FFA), the following composition was selected: C16:0, C18:0, C20:0, C22:0, C23:0, C24:0 and C26:0 at molar ratios of 1.8, 4.0, 7.7, 42.6, 5.2, 34.7 and 4.1 respectively. This chain length distribution is based on a FFA composition in SC (9). To achieve lipid mixtures at an equimolar CHOL:synthCER:FFA composition appropriate amounts of individual lipids were dissolved in chloroform : methanol (2:1). After evaporation of the organic solvent under a stream of nitrogen, the lipid mixtures were re-dissolved in hexane : ethanol (2:1) at a lipid concentration of 4.5 mg/ml. In some studies the protonated FFA were replaced by the deuterated FFA using a slightly different FFA composition, namely DFFA(5) with C16, C18, C20, C22 and C24 at molar ratios of 1.8, 4.0, 7.6, 47.8 and 38.8 respectively.

2.3.2 Spraying of SCS with an airbrush

An evolution solo airbrush (Airbrush Service Almere, The Netherlands) connected to gaseous nitrogen was used to spray the lipid mixtures onto a polycarbonate filter disk with a pore size of 50 nm. For the manual spraying of SCS the same procedure is followed as published

previously (11, 12). For spraying multiple SCS simultaneously, the airbrush was equipped with an automated rotor developed by the fine mechanical and electronics department of our university, see figure 1 for a schematic presentation.

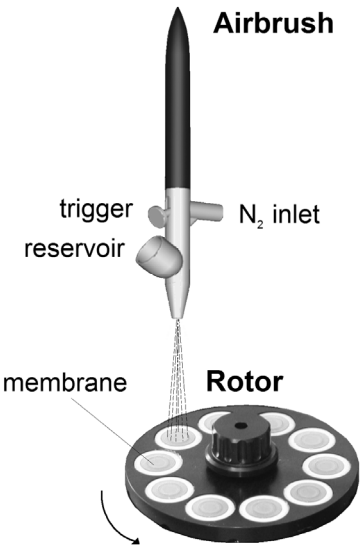

Figure 1: Schematic representation of the airbrush equipped with a rotor that contains ten filters. The rotor cap, mechanics and electronics are not shown. The airbrush is filled with lipid solution and under a stepping rotation the filters are sprayed up to a 1000 times in total.

The rotor can contain up to ten SCS filters and rotates the filters under the airbrush nozzle in a continuous stepping movement. The spraying is automatically discontinued during each movement of the rotor. The rotor is covered by a cap with a circular opening positioned exactly below the nozzle at a distance of 7.7 cm. The nozzle and the cap are not rotating but held in the same position. In this way only 1 filter positioned below the opening is sprayed, while the other filters are protected from dust by the cover. Due to the rotating movement all filters are sprayed sequentially. A nitrogen stream

is flowing underneath the cap to dry the SCS after each spray. The filters are sprayed on average around 70 to 100 times per SCS, depending mainly on the volume of lipid solution inserted which varies between 500 to 800 µl per SCS. The drying period (between sprays) is 16 s per SCS and the spray-time is 1.5 s per SCS. The (N_2) spray pressure is ~1.09 bar.

2.3.3 Spraying of SCS with a modified Linomat

A Linomat IV (Camag, Muttenz, Switzerland) was extended with a y-axis arm developed by the fine mechanical and electronics department of our university. The linomat device makes use of a Hamilton syringe (100 µl) and mechanics to spray a confined (programmable) volume of sample solution from a distance of ~1 mm to the porous filter substrate. With the y-axis in use, the linomat is capable of spraying lipids in a rectangular shape, by a continuous zigzag movement. The linomat sprays the lipid solution with a flow of 5.0 µl/min at a movement speed of 1.01 cm/s in a square of 8 x 8 mm. The amount of lipid solution used is ~200 µl per SCS. Therefore in 40 minutes it covers the circular diffusion area (of 6 mm diameter).

2.3.4 Equilibration of SCS

After spraying with the manual/rotor airbrush or linomat, the lipid-loaded filters were equilibrated at 70°C or 80°C for a period of at least 10 minutes and subsequently cooled down to room temperature in approximately 30 min.

2.4 SCS lipid composition and distribution

The lipid composition and distribution was determined by two methods. One-dimensional high performance thin layer chromatography (HPTLC) was used to establish the distribution of the various lipid classes over the filter surface. Briefly, the lipid-loaded filters were cut into two circular parts: the centre (diameter 4 mm; area 12.6 mm^2) and the periphery (diameter 9 mm; area 51.0 mm^2) as shown in figure 2. The lipids were

extracted in 0.5 ml chloroform : methanol (2:1) by extensive vortexing and were subsequently dried under a nitrogen flow and re-dissolved in chloroform : methanol to obtain an equal lipid concentration for the two fractions. Aliquots were applied on a silica plate (Merck, Darmstadt, Germany) under a flow of nitrogen using a linomat. After eluting with different organic solvent mixtures (15), the silica plate was sprayed with copper sulphate.

A Bio-Rad FTS4000 Fourier transform infrared spectrometer (FTIR) (Cambridge MA, USA) equipped with a broad-band mercury cadmium telluride detector, cooled with liquid nitrogen, was used to measure the infrared absorption of SCS with perdeuterated FFA. The spectra were collected in transmission mode as a co addition of 64 scans at 4.0 cm^{-1} resolution. All samples were measured at room temperature under continuous dry air purge.

In order to be able to obtain a local absorption spectrum from a well defined small region in the membrane a pinhole of 1.4 mm in diameter (developed by the fine mechanical department) was designed and used to measure a spectrum at five positions on the SCS (see figure 3A). From the peak integration of the CH_2 and CD_2 stretching vibrations at 2849 and 2088 cm^{-1} respectively, the absorption spectra intensity ratio between CER and perdeuterated FFA could be obtained for each position. A change in intensity ratio indicates a change in CER/FFA composition.The contribution of CHOL to the vsCH_2 vibration is neglected because of its much shorter lipid tail. All samples were measured at room temperature.

2.5 Thickness and lateral organization of the SCS lipid layer

In order to determine the thickness of the SCS by the absorption in the FTIR spectrum, first the relation between the infrared absorption and layer thickness was determined. For this purpose the spraying speed of the linomat was lowered, so that a complete SCS is sprayed in 17 homogeneous layers. The FTIR spectrum in the center of the SCS was measured through

the pinhole after each additional sprayed layer with the linomat. After each measurement the FTIR absorption was calculated from peak integration of the CH_2 rocking vibration ($\rho_r CH_2$ at 720 cm^{-1}). After the relationship between the FTIR absorption and the layer thickness was established, the infrared absorption of the CH_2 rocking vibration was used as a parameter to determine the uniformity of the SCS thickness. The pinhole was set at the center and at 1 and 2 mm radial distance from the center (see figure 3A). Subsequently the FTIR spectrum was measured and absorption was determined using the $\rho_r CH_2$ at 720 cm^{-1}.

From the same FTIR spectrum also the packing of the lipids can be determined. This information is provided by the CH_2 scissoring vibrations (δCH_2) around 1467 cm^{-1}. In addition the SCS was prepared with perdeuterated FFA. This allows determining whether FFA and CER participate in one lattice. This information can be obtained from the CD_2 scissoring mode (δCD_2). The contour of this band is located at approximately 1088 cm^{-1}. All FTIR measurements were performed at room temperature.

2.6 Lipid Loss during spraying

For the airbrush and linomat preparation methods the lipid yield on the filter surface was determined. After spraying, the membrane was weighed and the empty membrane weight was subtracted. The resulting lipid layer weight (after spraying) was divided by the amount of lipids used during spraying multiplied by 100%, to obtain the percentage lipid yield on the filter. Also, the yield inside the diffusion area was determined. After spraying and equilibration, the circular membrane diffusion area of 6 mm diameter was punched and weighed, the empty membrane weight was subtracted. The remaining lipid weight was again divided by the amount of lipids used during spraying and multiplied by 100% to obtain the percentage lipid yield inside the diffusion area on the filter.

2.7 Lamellar organization and orientation determined by SAXD

Small-angle X-ray diffraction was used to acquire information about the lamellar organization (i.e., the repeat distance of a lamellar phase) and the orientation of the lamellae. The scattering intensity I (in arbitrary units) was measured as a function of the scattering vector q (in reciprocal nm). The latter is defined as $q=(4\pi\sin\theta)/\lambda$, in which θ is the scattering angle and λ is the wavelength. From the positions of a series of equidistant peaks (q_n), the periodicity, or d-spacing, of a lamellar phase was calculated using the equation $q_n=2n\pi/d$, n being the order number of the diffraction peak. One dimensional intensity profiles were obtained by transformation of the 2D SAXD pattern from Cartesian (x,y) to polar (ρ,θ) coordinates and subsequently integrating over θ from 60 to 120 degrees. All measurements were performed at the European Synchrotron Radiation Facility (ESRF, Grenoble) using station BM26B (16). The X-ray wavelength and the sample-to-detector distance were 0.124 nm and 1.6 m, respectively. Diffraction data were collected on a two-dimensional multiwire gas-filled area detector with 512×512 pixels of 0.25 mm spatial resolution. The spatial calibration of this detector was performed using silver behenate (d=5.838 nm). A filter with lipid layers was mounted parallel to the primary beam in a temperature controlled sample holder with mica windows. Static diffraction patterns were collected at room temperature. The temperature-induced phase changes were measured by collecting successive diffraction patterns, while the temperature of the sample was raised from 20 to 80°C at a rate of 1°C/min, subsequently kept at this temperature for 10 min and then reduced in temperature to 20°C at a rate of 5°C/min. During the dynamic measurements each diffraction curve was collected for a period of 2 min.

2.8 Diffusion studies on human SC and SCS

In vitro permeation studies were performed using Permegear in-line diffusion cells (Bethlehem PA, USA) with a diffusion area of 0.28 cm^2. SC on a supporting dialysis membrane (5000 Da, apical side facing the donor

chamber) or the SCS was mounted in the diffusion cell and was hydrated for 1 h in phosphate buffered saline (PBS: NaCl, Na_2HPO_4, KH_2PO_4 and KCL in MQ water with a concentration of 8.13, 1.14, 0.20 and 0.19 g/l respectively) at pH 7.4 prior to the experiment. The donor compartment was filled with 1400 μl of benzoic acid solution in PBS (pH 7.4) at a 2.0 mg/ml concentration. Benzoic acid has a log $P_{oct/water}$ value of 1.9. The acceptor phase consisted of PBS (pH 7.4), which was flushed at a flow rate of about 2 ml/h. The acceptor phase was stirred with a magnetic stirrer. The exact volume per collected fraction was determined by weighing. Each experiment was performed under occlusive conditions, by closing the opening of the donor compartment with adhesive tape. The temperature of the SC or SCS was maintained at ~32ºC during the total length of the experiment, using a thermo-stated water bath. Fractions were collected for 18 h at a 1 h interval. Diffusion studies were performed on SCS from the manual airbrush, rotor airbrush and linomat method, as well as SCS equilibrated at 70 and 80ºC. Steady state fluxes and lag-times were determined from a plot of the cumulative permeated amount. The steady state flux is the slope of the linear part of this graph. The lag-time is determined by regression of this linear part to the time at y=0.

3. Results

The SCS was constructed with the three methods; the manual airbrush method used in previous studies, the automated rotor airbrush method and the linomat method. In order to characterize the SCS, the lipid composition and distribution, membrane thickness, lipid yield, lipid organization, and the barrier function of the SCS prepared by the different methods have been examined.

3.1 Lipid composition and distribution

In order to determine the uniformity of the lipid composition along the surface of SCS, HPTLC and FTIR are employed. Using HPTLC, the mean lipid composition of the inner and outer ring of the SCS is examined. The results are provided in figure 2. From this figure it is obvious that no differences in lipid profile are observed between inner and outer ring of SCS prepared by the manual airbrush, rotor airbrush and linomat. This indicates that the mean lipid composition and distribution in the central and peripheral part of the SCS manufactured by the three methods is similar.

More detailed information about the fluctuations in FFA/CER ratio at various positions along the SCS surface is obtained by using FTIR.

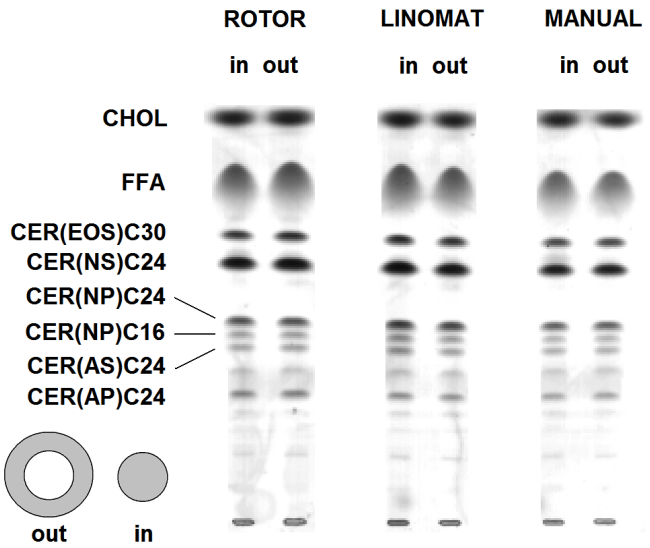

Figure 2: HPTLC pattern of the center part (in) and outer ring (out) of SCS prepared with the three methods. No differences in lipid composition are visible between inner and outer membrane.

When using deuterated FFA, in the FTIR spectrum the fluctuations in ratio of peak intensities of $vsCH_2$ (located at 2849 cm^{-1}) and $vsCD_2$ (located

at 2088 cm^{-1}) is directly related to the fluctuations in molar ratios of the protonated CER and deuterated FFA chains, respectively. A change in the integrated peak ratio of $vsCH_2$: $vsCD_2$ is indicative for a change in the molar ratio of the protonated and deuterated chains. The integrated $vsCH_2$: $vsCD_2$ peak ratios of the five selected locations (see figure 3A) are shown in table 1, for SCS prepared with the manual-, rotor airbrush and linomat method. For each preparation method, the variation in $vsCH_2$: $vsCD_2$ peak ratio (between the different locations at the SCS) is very low, demonstrating a uniform CER : FFA ratio within the five selected positions. However, for the manual airbrush and linomat method, between SCS (at each position), a larger standard deviation for the $vsCH_2$: $vsCD_2$ peak ratio was observed than for the rotor method. This can be explained by the fact that the SCS from the rotor airbrush are all prepared simultaneously in one run, resulting in a very reproducible thickness of the SCS.

Table 1:
$vsCH_2$/$vsCD_2$ ratio measured at 5 positions (see also figure 3A) on SCS prepared with the three methods.

position	1	2	3	4	5
Rotor SCS (n=3)	3.20 ±0.02	3.18 ±0.02	3.16 ±0.04	3.23 ±0.05	3.26 ±0.07
Linomat SCS (n=3)	2.5 ±0.2	2.5 ±0.2	2.4 ±0.2	2.5 ±0.2	2.6 ±0.2
Manual SCS (n=3)	2.5 ±0.2	2.3 ±0.3	2.3 ±0.2	2.3 ±0.3	2.5 ±0.2

3.2 Thickness and cross section of the lipid layer

A uniform thickness of the lipid layer of the SCS is important when performing permeation experiments. In order to determine the SCS thickness at a predetermined position in the SCS, first a linear relation between the peak intensity of the $\rho_r CH_2$ rocking vibration at 720 cm^{-1} in the FTIR spectrum and the number of sprayed layers was determined. After each layer sprayed with the linomat, the IR absorption was determined by FTIR. The results are displayed in figure 3B. The graph clearly shows that

there is a linear relationship between the layer thickness of the SCS, expressed by the number of layers sprayed with the linomat, and its infrared absorbance around 720 cm^{-1} (the contours of the $\rho_r CH_2$ rocking vibration). Thus, by measuring the intensity of the $\rho_r CH_2$ mode, the relative thickness of a prepared membrane can be determined.

Using the linear relationship between the intensity of the absorption peak of the $\rho_r CH_2$ rocking vibration and the membrane thickness, the homogeneity in thickness of the lipid layer of SCS can be determined by measuring this $\rho_r CH_2$ rocking vibration intensity at various selected locations on the stratum corneum substitute. These locations are chosen in a cross section at the center and 1 and 2 mm out of the center. Figure 3C shows the relative infrared absorbance of the $\rho_r CH_2$ contour at the various positions on SCS, in which the intensity of the $\rho_r CH_2$ contour in the center of the membrane is set to 100%. From this figure it is obvious that for all three methods the layer thickness is highest in the center of the SCS and reduces towards the edge of the diffusion area. Furthermore, the linomat method delivers SCS with a more homogeneous layer thickness than SCS prepared with the rotor- or manual airbrush method.

3.3 Lipid loss during spraying

The distance between the nozzle and the supporting membrane using the airbrush method is 7.7 cm for the rotor and 5 to 10 cm for the manual holder, while the distance between the needle tip and the supporting membrane using the linomat method is only 1 mm. This may result in differences in lipid loss. Therefore the lipid yield in the diffusion area of the membrane is determined by weighing. For the manual airbrush, rotor airbrush and the linomat method, the recovery of lipids sprayed on the filter is respectively 68±19% (n=3), 52±4% (n=5) and 93±4% (n=3) of the total amount of lipids used for spraying. However, the recovery of lipids inside the diffusion area is 8±1% (n=4) for the manual airbrush, 10±1% (n=4) for the rotor airbrush and 31±2% (with n=13) for the linomat method. The recovery

in the diffusion area is less than the total recovery because a relatively small area of the membrane is used for diffusion. From these results it is clear that the airbrush method has a much lower lipid yield than the linomat preparation method.

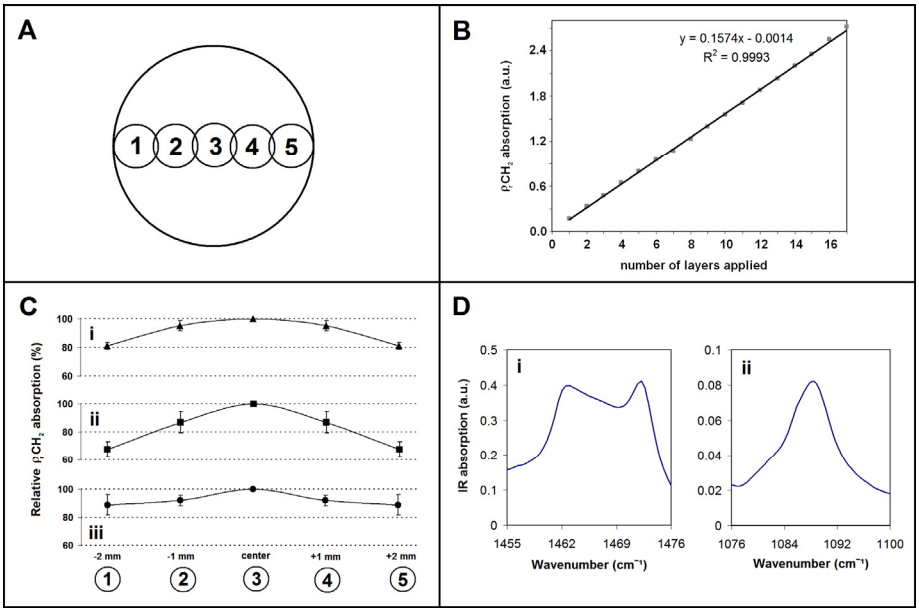

Figure 3: Overview of FTIR results. A) The five positions on SCS that were selected for the FTIR absorption measurements for determining variations in membrane thickness and DFFA/CER absorption ratio. B) The peak intensity of the FTIR rocking mode (ρrCH2) is plotted as function of the number of lipid layers sprayed with the linomat application method. A linear relationship is observed. C) Lipid layer cross section of SCS prepared with the rotor airbrush (i), manual airbrush (ii) and linomat (iii) (n=3 per method). The profile is calculated using the correlation between peak intensity and membrane thickness shown in B). The positions of the measurements are provided in (a). D) (i) Typical CH_2 scissoring mode in the FTIR spectrum obtained for SCS prepared with the three spraying methods. A doublet is observed with absorption maxima at 1463 and 1472 cm-1 indicative for the presence of an orthorhombic lateral packing. (ii) typical CD_2 scissoring mode for SCS with perdeuterated FFA. A singlet is observed with maximum at 1088 cm-1 indicative for participation of FFA and CER in one lattice.

3.4 Lipid packing

Information on the lipid packing can be obtained from the δCH_2 contours in the FTIR spectrum. If the δCH_2 band is a singlet at around 1467 cm^{-1}, the lipids form either a liquid or a hexagonal packing. However, when lipids form an orthorhombic packing, chains in scissoring mode interact via a short-range coupling resulting in splitting of the δCH_2 vibration known as factor group splitting**.** As a consequence the contour is a doublet located between 1463 cm^{-1} and 1473 cm^{-1}. The spectrum of the δCH_2 mode representative for SCS is provided in figure 3D-i. This spectrum reveals a doublet at 1463 and 1472 cm^{-1} respectively with a weak singlet around 1467 cm^{-1}. No difference in the scissoring contours was observed between SCS prepared using the different methods. Therefore, in SCS membranes the lipid packing is mainly orthorhombic with a small population of lipids forming a hexagonal packing.

When the FFA is replaced with deuterated FFA, information on the mixing of FFA and CER in one lattice can be obtained. If CER and deuterated FFA participate in one lattice, decoupling takes place and the doublet in the δCD_2 mode (present in a mixture with only deuterated FFA) changes into a singlet at 1088 cm^{-1} in the CER:CHOL:FFA(deuterated) mixtures (17). The δCD_2 band typical for SCS prepared with any of the three methods is shown in figure 3D-ii. A singlet was observed at all five positions (see figure 3A) on the SCS indicating that deuterated FFA and CER participate in the same crystal lattice.

3.5 Lamellar organization and orientation

Besides the lateral organization (lipid packing), the formation of the lamellar phases and their orientation are both assumed to be crucial for the skin barrier function. The lamellar organization is examined by small angle X-ray diffraction using a two-dimensional detection. Figure 4A shows a typical two-dimensional X-ray diffraction pattern of the lipids in the SCS

prepared with the linomat method. Equal patterns have been acquired for SCS prepared with the other two methods. The high intensity at the meridian (see arrow in figure 4A) demonstrates that the lipid lamellae have a preferred orientation parallel to the surface of the SCS.

In figure 4B the intensity profile of the integrated SAXD pattern is plotted. From the position of the diffraction peaks two lamellar phases can be identified with repeat distances of 11.6 and 5.4 nm. The diffraction orders 1 to 4 of the long periodicity phase (LPP, with d = 11.6 nm) are located at q = 0.54, 1.10, 1.62 and 2.15 nm^{-1} respectively. The 1st and 2nd order of the short periodicity phase (SPP, with d ~ 5.7 nm) are located at q = 1.10 and 2.15 nm^{-1}. Besides the two lamellar phases, phase separated CHOL could be identified by the peaks located at q = 1.86 and 3.73 nm^{-1}.

Finally two peaks are observed at q = 1.43 and 2.86 nm^{-1}, which should be assigned to another lipid structure. As these peaks were never identified in the diffraction pattern of stratum corneum (7, 18, 19), additional studies were performed to observe whether the formation of this phase could be avoided. One of the critical parameters is the elevated equilibration temperature after spraying. Therefore, for an unequilibrated SCS (prepared by the linomat method), the phase behavior was examined as a function of temperature during heating and cooling. The result is provided in figure 4C. The measurement starts at room temperature, and upon heating, between 70 and 80ºC all diffraction peaks disappear. After the SCS is kept at 80ºC for 10 minutes (equilibration), the SCS is cooled down to 20ºC at a rate of 5°C/min. During this cooling process, first a diffraction peak attributed to the SPP (at q = 1.2 nm^{-1}) as well as the CHOL peak appear around 60°C, and at slightly lower temperature also the diffraction peaks of the LPP appear. Interestingly, this thermal treatment did not result in the reappearance of the peaks attributed to the 4.4 nm phase. In a similar dynamic experiment an unequilibrated SCS was equilibrated at 75 instead of 80ºC, it was striking that the diffraction peak at 4.4 nm and the CHOL peak did not disappear at 75ºC and were still present after equilibration (data not shown).

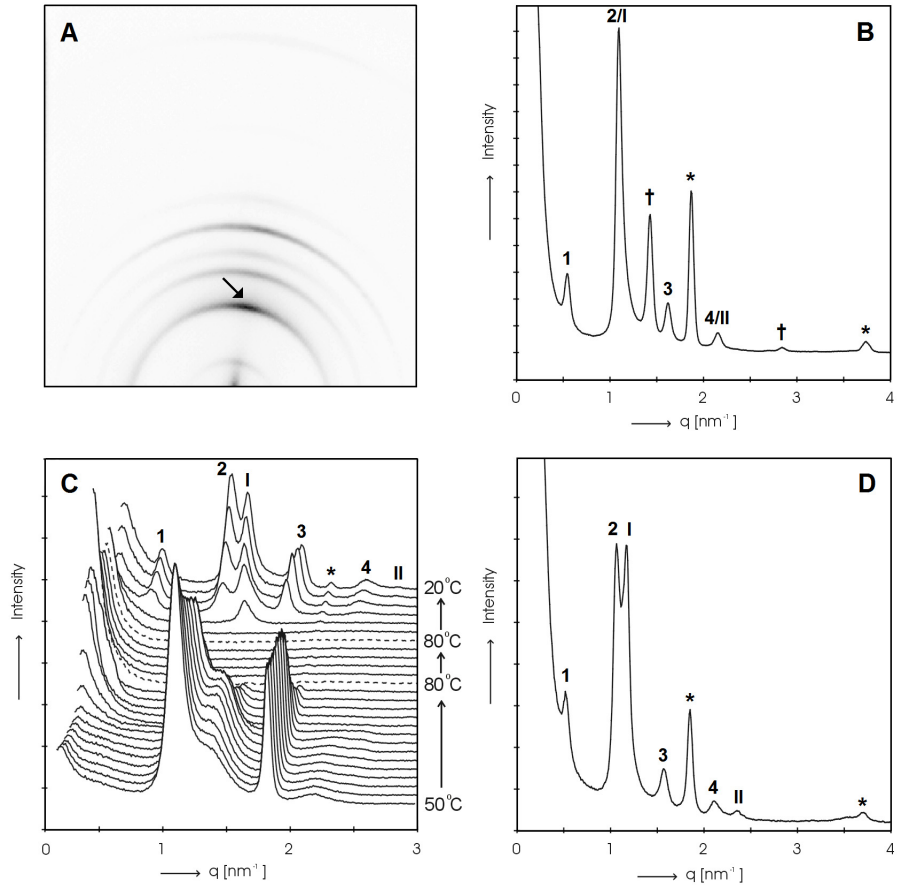

Figure 4: Overview of SAXD results. A) Typical 2D SAXD pattern of SCS equilibrated at 70ºC. The arrow denotes the position of the intensity maximum. B) Intensity profile of integrated SAXD pattern of SCS equilibrated at 70ºC. The orders attributed to the LPP are located at q-values of 0.54 (1st order), 1.10 (2nd order), 1.62 (3rd order) and 2.15 nm^{-1} (4th order). The 1st and 2nd order peak of the SPP (indicated by I and II) are located at q-values of 1.10 and 2.15 nm^{-1}. The asterisk (*) indicates the reflections of crystalline cholesterol (q values at 1.86 and 3.74 nm^{-1}) and † denotes the two reflections attributed to the additional phase with a periodicity of 4.4 nm (q values at 1.43 and 2.83 nm^{-1}). C) Intensity profiles as a function of temperature. The X-ray diffraction profile has been measured from 50 to 80ºC, equilibrated during 10 minutes and subsequently cooled with a cooling rate of 5ºC/min. In heating, between 75 and 80ºC all ordering disappears. In the cooling process, between 70 and 50ºC the LPP and SPP are formed. D) X-ray diffraction profile of SCS equilibrated at 80ºC. The orders 1 to 4 of the LPP are located at q = 0.52, 1.06, 1.57 and 2.11 nm^{-1}, the orders I and II of the SPP are located at q = 1.17 and 2.35 nm^{-1}). After equilibration at 80ºC the additional phase is not formed and the spacing of the LPP is longer as compared to the LPP in (A). This is clearly visible by the split peaks at the first order of the SPP and second order LPP in (D).

For this reason, in preparing SCS, it was decided to adapt the equilibration temperature from 70 to 80ºC. Figure 4D shows the SAXD pattern of SCS (prepared by the linomat method) after equilibration at 80ºC; it is obvious that the 4.4 nm phase disappeared and the intensity of the first order cholesterol peak reduced, in comparison with SCS equilibrated at 70ºC (figure 4A). Furthermore, the repeat distance of the long periodicity phase increased to 12.2 nm more closely mimicking the lipid organization in stratum corneum.

As a clear difference in phase behavior was observed when equilibrating the SCS at 70 or 80ºC, polarization microscopy was conducted to study the presence of crystals at the two equilibration temperatures. In figure 5 two typical polarization microscopic images are shown for SCS equilibrated at 70ºC and 80ºC. It can be seen that the degree of mosaicity is greatly reduced at 80ºC, while at 70ºC needle-shaped crystals are present. Because the cholesterol fraction is reduced with a temperature rise from 70ºC to 80ºC (as concluded from SAXD results), the needle-shaped crystalline domains observed at 70ºC may originate from phase separated cholesterol. This hypothesis was further investigated with SCS prepared with a reduced cholesterol content (molar ratio of CER/CHOL/FFA = 2/1/2). This SCS equilibrated at 70ºC indeed showed a lower number of crystals than SCS prepared using equimolar CER:CHOL:FFA mixtures (images not shown).

3.6 Variation in equilibration temperature and permeation properties

As a difference in lipid organization was observed when equilibrating the SCS at 70ºC or 80ºC, it was decided to perform permeation studies using SCS equilibrated either at 70 or 80ºC. In figure 6A the permeation profiles of benzoic acid are depicted of SCS prepared at 70 or 80ºC using either the linomat or rotor method.

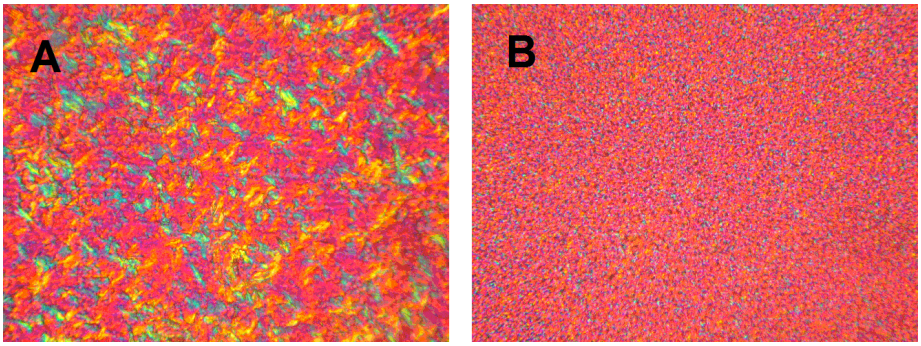

Figure 5: Transmission polarization images (40x magnification) of SCS equilibrated at 70ºC (A) and SCS equilibrated at 80ºC (B). The mosaicity due to cholesterol crystals is drastically reduced at 80ºC.

When the SCS is equilibrated at 80ºC, the lag-time (τ) is 1.2 ± 0.2 h, while equilibration at 70ºC results in a τ of 3.4 ± 0.8 h.Furthermore, the steady state flux across SCS equilibrated at 70ºC is 18 ± 1 μg/cm^2/h which is significantly lower than the steady state flux across SCS equilibrated at 80ºC were J_{ss} = 25 ± 2 μg/cm^2/h. In an additional series of studies the benzoic acid flux across the SCS prepared with the different methods has been determined and compared to that across SC. The SCS were all equilibrated at 80ºC, the fluxes are shown in figure 6B. It can be seen that the permeation profiles of SCS prepared with the three methods are very similar to each other. Furthermore, the steady state flux of the SCS closely resembles the steady state flux of human SC; the J_{ss} are on average 24 ± 2 μg/cm^2/h for SCS and 22 ± 3 μg/cm^2/h for SC. The lag-time is shorter for SC than for the SCS; τ is -0.1 ± 0.3 h for SC and 1.1 ± 0.5 h for SCS.

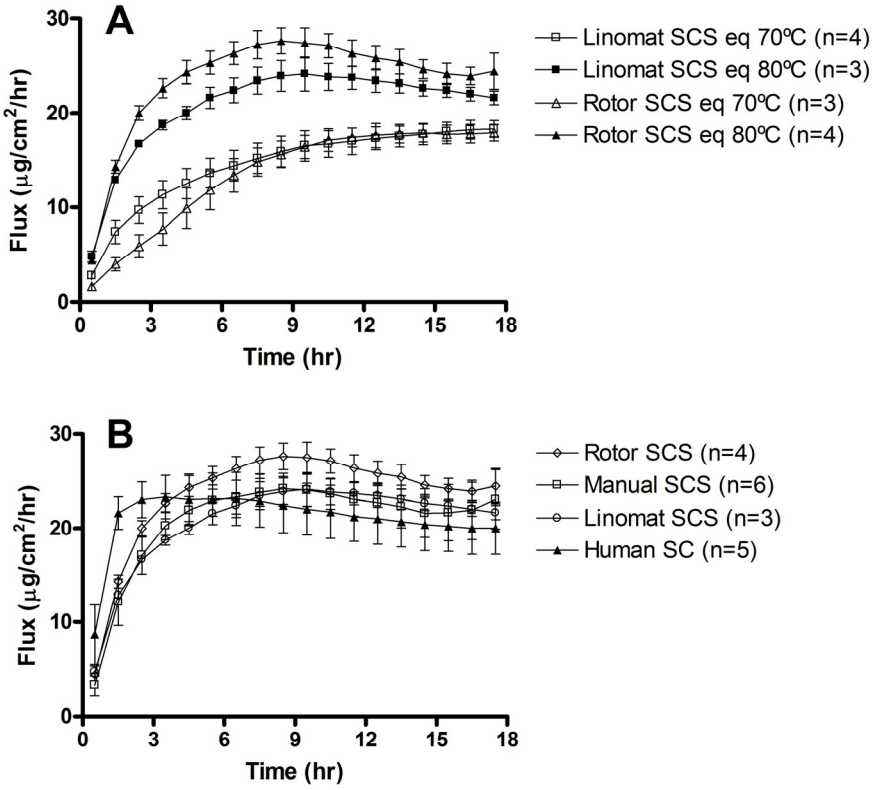

Figure 6: Permeation studies at 32ºC on SCS with benzoic acid used as model drug. (a) SCS previously equilibrated at 70ºC and 80ºC (two preparation methods) and (b) SCS (pre-eq. at 80ºC) prepared with the three methods, compared to human SC. SCS equilibrated at 80ºC displays a shorter lag-time and higher steady state flux than SCS equilibrated at 70ºC. The three different methods for preparing SCS result in very similar diffusion profiles, with a steady state flux comparable to h uman SC, however with a larger lag-time than SC.

4. Discussion

The main purpose of our studies is to construct a SCS that can be used as an in vitro permeation model. This is of interest for at least two

reasons. First, the SCS can serve as a model for human stratum corneum to screen compounds on their skin permeability or study the effect of formulations on the permeation profile. Second, the SCS offers the unique opportunity to study the relationship between lipid composition, lipid organization and permeability in one model. This is of particular importance for understanding the reduced skin barrier function in diseased skin. For screening purposes several reconstructed skin models are already commercially available. However, although these models are very useful for skin irritation tests (20, 21), they show an impaired barrier compared to human skin. This makes these models less attractive as an alternative for human skin in permeation studies (22), (23).

When used for permeation purposes, the SCS should i) be prepared in a very reproducible manner, ii) be homogeneous in composition and in membrane thickness and iii) mimic lipid organization and orientation of human SC. These properties of SCS, and its permeation properties, will be discussed below.

4.1 Optimal preparation with the linomat method

In our present study, besides the manual airbrush and rotor method, the linomat method was used to prepare the SCS. Kuempel et al also used the linomat for spraying lipids on a Millipore filter disk (24) and they showed for the first time that it is possible to form the broad-narrow-broad pattern characteristic for SC lipid organization using RuO_4 staining. However, their studies were different from ours in at least three aspects. i) Kuempel et al used total lipid extracts of pig SC without isolation of the CER, while we use mixtures based on synthetic CER. As we noticed in previous studies, the preparation method of mixtures prepared with synthetic CER is different from that prepared with isolated CER, especially with respect to the choice of the optimal equilibration temperature (14). ii) Kuempel et al did not modify the linomat by adding an extra arm, which allows spraying of lipids in a predefined area of the supporting membrane. This may indicate that their

supporting membrane is not homogeneously covered with lipids. This limits the use of these membranes in permeation studies. iii) Kuempel et al concluded that in the absence of hydration no broad-narrow-broad structure (visualized by RuO_4 staining) could be obtained. The latter is likely correlated with the formation of the LPP. Using our application method it is possible to form the LPP in the absence of water. Furthermore, in our previous study we showed that hydration at elevated temperature results in phase separation between lipid and water domains in the membrane (12) creating a leaky SCS, which cannot be used in permeation studies.

The linomat application method showed some advantages above the rotor and manual air-brush spraying methods. First, the loss of lipids for the linomat method was much lower than for the airbrush spraying methods, which is most probably due to the shorter nozzle to membrane distance. Second, the membrane thickness is more uniform using the linomat application method instead of the airbrush spraying methods.

HPTLC and the ratio of the absorption of the CH_2/CD_2 symmetric stretching frequencies in the FTIR spectrum both revealed that in all SCS the lipid composition parallel to the SCS surface is quite homogeneous. However, in contrast to the rocking frequencies used to determine the SCS thickness, the CH_2 and CD_2 stretching absorptions used to determine the uniformity of the SCS composition, are not linearly correlated with the SCS thickness. The signal of the MCT detector used to measure the infrared spectra is nonlinear with sample absorption in the region around 2800 cm^{-1}, which is the region of the CH_2 stretching mode used to determine CH_2/CD_2 ratio and thus the lateral homogeneity in the lipid membrane. Therefore, a variation in membrane thickness (different absorption) in this region, will affect to some extent the CH_2/CD_2 intensity ratio of the stretching mode. The membranes prepared by the rotor airbrush method were thinner than those prepared by the linomat and manual rotor method, which resulted in higher CH_2/CD_2 stretching peak ratios of the SCS prepared by the rotor airbrush method, see table 1.

4.2 FTIR as a non-destructive tool to measure thickness and lipid distribution

The average membrane thickness and cross section of the lipid layer are assessed by FTIR without destruction of the SCS. This makes it an elegant method for quality control of prepared SCS as the measurements can be performed prior to a permeation study. Another control is the assessment of lipid distribution by FTIR using perdeuterated fatty acids. If the distribution of lipid components over the membrane surface is not uniform, the LPP that is crucial for the barrier function (11), may not be formed.

Pidgeon et al demonstrated already in 1989 that FTIR can be used to quantify the lipid content in organic lipid solutions and extracted membrane preparations (25). Although our method presented in this paper is based on the method of Pidgeon, there are some differences. We quantify the lipid thickness of the SCS by integration of the peak intensity of the rocking vibration, whereas Pidgeon used an internal standard combined with the stretching vibrations. We did not choose for an internal standard as this might affect the lipid organization and therefore the permeability of the SCS. Also, we chose for the rocking vibrations because we observed that only in this region of the spectrum the absorption was linear with the lipid quantity.

Furthermore, it is well known that the steady state flux of a substance through a membrane according to Fick's Law is linear dependent on the reciprocal membrane thickness. Therefore a homogeneous reproducible thickness is a prerequisite for the SCS when used in screening studies. Variation in thickness of the SCS prepared with the two airbrush methods is larger than that of the SCS prepared by the linomat method, although even when using the linomat method there is still a small variation in thickness. This may be due to the equilibration step at elevated temperatures. At these temperatures the lipids are in the hexagonal to liquid phase transition, which will result in a small additional spreading over a larger surface area.

4.3 The SCS closely mimics the stratum corneum lipid organization

In human SC the lipids are organized mainly in an orthorhombic lateral packing, which is considered to play an important role in the skin barrier function (26-28). Therefore, it is a prerequisite that the SCS form an orthorhombic (very tight) lateral lipid packing. As demonstrated in figure 3D-i, the lipids form the orthorhombic lateral packing. Furthermore, as the inter peak distance of the doublet is approximately 9.2 cm^{-1} approaching the maximum splitting of 11 cm^{-1}, this indicates that the crystalline domain sizes exceed that of 100 lipids (29). In previous studies, FTIR was used to study the mixing properties of perdeuterated palmitic acid and protonated CER in one lattice (29, 30). In the study of Moore et al, palmitic acid and bovine brain CER type III form their own separate orthorhombic phases. This contrasts our finding that FFA and CER participate in one lattice. Their model however was less complex than ours, with only 3 lipid components: a single CER, CHOL and palmitic acid. The smaller number of components in that mixture may facilitate phase separation.

Not only the orthorhombic packing, but also the LPP has been suggested to be important for the barrier function (11). The diffraction pattern of the SCS shows the coexistence of the LPP and SPP, similarly as in human SC. However, after equilibration of the SCS at 70ºC an additional unknown phase was formed not present in SC. This phase disappeared after using an equilibration temperature of 80ºC. This is in contrast to the phase behavior of lipids casted on mica in previous studies, in which an equilibration temperature of 70ºC was sufficient (14). Very recently, we observed that the solvent choice for spraying lipids accounts for the difference in required equilibration temperature. When sprayed on mica, the lipids dissolved in chloroform:methanol (2:1 v/v) form the LPP and SPP, while the lipids dissolved in hexane:ethanol (2:1 v/v) result in formation of the additional unknown phase (data not shown). Most probably, when using hexane:ethanol (2:1 v/v) some lipid components are dissolved less readily,

which results in a crystallization of these components forming separate lipid domains during the spraying process.

In the two-dimensional detection plane, the arc-shaped form of the reflections in the diffraction pattern in figure 4A indicates that the majority of the lamellae are oriented parallel to the surface of the membrane. This arc-shaped pattern is very similar to that observed for SC (not shown) indicating that the SCS has a very similar lamellar orientation.

4.4 SCS as a permeability model can replace human SC

For our permeation studies we chose a model compound similar to the compounds used previously (11), namely benzoic acid (BA). As we observed differences in the phase behavior after equilibration at 70 and 80°C we have first investigated the effect of equilibration temperature on the permeability of SCS. It appeared that for the lower equilibration temperature of 70ºC (where a separate phase exists) the SCS permeability for BA is slightly lower and the lag-time longer. Equilibration at 80ºC resulted in a shorter lag-time, which mimics more closely the diffusion profile across human SC. This demonstrates that it is important to mimic the lipid phase behaviour in SC as closely as possible.

Subsequently, the SCS were prepared with all three methods and after equilibration at 80ºC their permeability was compared to SC. No significant differences in BA permeability were observed regardless of the preparation method used. Although the diffusion profiles through the SCS revealed a slightly longer lag-time than the diffusion profiles through SC, the steady state fluxes through SCS were very similar to those through SC. Therefore, the SCS can serve as an excellent permeability model and replace stratum corneum in diffusion studies.

In conclusion, in this study it has been shown that the preparation of SCS is feasible with any of the tested preparation methods; manual airbrush, rotor airbrush or linomat. The SCS prepared with the three methods

displayed the desired properties of a uniform lipid composition, the presence of an orthorhombic lateral organization, the distinct phases with a lamellar orientation approximately parallel to the membrane surface and permeation properties similar to human SC. The linomat method was selected as the most appropriate method for preparing the SCS, as the spraying was most efficient and the membrane thickness was more uniform compared to the two airbrush methods.

Acknowledgements

We would like to thank the company Cosmoferm B.V. for the provision of the synthetic ceramides, our fine mechanical department and our electronics department of Leiden University for the development of the airbrush setup and modifications to the linomat and diffusion setup. The Netherlands Organization for Scientific Research (NWO) is acknowledged for the provision of the beam time and we thank the personnel at the DUBBLE beam line 26 at the ESRF for their support with the x-ray measurements, as well as the group of crystallography at the University of Amsterdam for additional x-ray measurements.

References

1. Simonetti, O., A. J. Hoogstraate, W. Bialik, J. A. Kempenaar, A. H. Schrijvers, H. E. Bodde, and M. Ponec. 1995. Visualization of diffusion pathways across the stratum corneum of native and in-vitro-reconstructed epidermis by confocal laser scanning microscopy. Arch. Dermatol. Res. 287:465-473.
2. Wertz, P. W., M. C. Miethke, S. A. Long, J. S. Strauss, and D. T. Downing. 1985. The composition of the ceramides from human stratum corneum and from comedones. J. Invest. Dermatol. 84:410-412.
3. Robson, K. J., M. E. Stewart, S. Michelsen, N. D. Lazo, and D. T. Downing. 1994. 6-Hydroxy-4-sphingenine in human epidermal ceramides. J. Lipid. Res. 35:2060-2068.
4. Stewart, M. E., and D. T. Downing. 1999. A new 6-hydroxy-4-sphingenine-containing ceramide in human skin. J. Lipid. Res. 40:1434-1439.
5. Ponec, M., A. Weerheim, P. Lankhorst, and P. Wertz. 2003. New acylceramide in native and reconstructed epidermis. J. Invest. Dermatol. 120:581-588.
6. Bouwstra, J. A., G. S. Gooris, J. A. van der Spek, and W. Bras. 1991. Structural investigations of human stratum corneum by small-angle X-ray scattering. J. Invest. Dermatol. 97:1005-1012.
7. Bouwstra, J. A., G. S. Gooris, W. Bras, and D. T. Downing. 1995. Lipid organization in pig stratum corneum. J. Lipid Res. 36:685-695.
8. Bouwstra, J., G. Gooris, and M. Ponec. 2002. The lipid organisation of the skin barrier: liquid and crystalline domains coexist in lamellar phases
   journal of Biological Physics 28:211-223.
9. Wertz, P. 1991. Epidermal lipids. In Physiology, Biochemistry and Molecular Biology of the Skin. L. A. Goldsmith, editor. Oxford University Press, Oxford. 205-235.
10. Motta, S., M. Monti, S. Sesana, R. Caputo, S. Carelli, and R. Ghidoni. 1993. Ceramide composition of the psoriatic scale. Biochim. Biophys. Acta 1182:147-151.
11. de Jager, M., W. Groenink, R. Bielsa i Guivernau, E. Andersson, N. Angelova, M. Ponec, and J. Bouwstra. 2006. A novel in vitro percutaneous penetration model: evaluation of barrier properties with p-aminobenzoic acid and two of its derivatives. Pharm. Res. 23:951-960.
12. de Jager, M., W. Groenink, J. van der Spek, C. Janmaat, G. Gooris, M. Ponec, and J. Bouwstra. 2006. Preparation and characterization of a stratum corneum substitute for in vitro percutaneous penetration studies. Biochim. Biophys. Acta 1758:636-644.

13. Bouwstra, J. A., G. S. Gooris, K. Cheng, A. Weerheim, W. Bras, and M. Ponec. 1996. Phase behavior of isolated skin lipids. J. Lipid Res. 37:999-1011.
14. de Jager, M. W., G. S. Gooris, M. Ponec, and J. A. Bouwstra. 2005. Lipid mixtures prepared with well-defined synthetic ceramides closely mimic the unique stratum corneum lipid phase behavior. J. Lipid. Res. 46:2649-2656.
15. Weerheim, A., and M. Ponec. 2001. Determination of stratum corneum lipid profile by tape stripping in combination with high-performance thin-layer chromatography. Arch. Dermatol. Res. 293:191-199.
16. Bras, W. 1998. An SAXS/WAXS beamline at the ESRF and future experiments. Journal of Macromolecular Science-Physics B37:557-565.
17. Gooris, G. S., and J. A. Bouwstra. 2007. Infrared spectroscopic study of stratum corneum model membranes prepared from human ceramides, cholesterol, and fatty acids. Biophys. J. 92:2785-2795.
18. White, S. H., D. Mirejovski, and G. I. King. 1988. Structure of lamellar lipid domains and corneocytes envelopes of murine stratum corneum. Biochemistry:3725-3732.
19. Bouwstra, J. A., G. S. Gooris, J. A. van der Spek, and W. Bras. 1991. Structural investigations of human stratum corneum by small-angle X-ray scattering. J Invest Dermatol 97:1005-1012.
20. Kandarova, H., M. Liebsch, E. Schmidt, E. Genschow, D. Traue, H. Spielmann, K. Meyer, C. Steinhoff, C. Tornier, B. De Wever, and M. Rosdy. 2006. Assessment of the skin irritation potential of chemicals by using the SkinEthic reconstructed human epidermal model and the common skin irritation protocol evaluated in the ECVAM skin irritation validation study. Altern. Lab. Anim. 34:393-406.
21. Tornier, C., M. Rosdy, and H. I. Maibach. 2006. In vitro skin irritation testing on reconstituted human epidermis: reproducibility for 50 chemicals tested with two protocols. Toxicol. In Vitro 20:401-416.
22. Schmook, F. P., J. G. Meingassner, and A. Billich. 2001. Comparison of human skin or epidermis models with human and animal skin in in-vitro percutaneous absorption. Int. J. Pharm. 215:51-56.
23. Netzlaff, F., C. M. Lehr, P. W. Wertz, and U. F. Schaefer. 2005. The human epidermis models EpiSkin, SkinEthic and EpiDerm: an evaluation of morphology and their suitability for testing phototoxicity, irritancy, corrosivity, and substance transport. Eur J Pharm Biopharm 60:167-178.
24. Kuempel, D., D. C. Swartzendruber, C. A. Squier, and P. W. Wertz. 1998. In vitro reconstitution of stratum corneum lipid lamellae. Biochim. Biophys. Acta 1372:135-140.
25. Pidgeon, C., G. Apostol, and R. Markovich. 1989. Fourier transform infrared assay of liposomal lipids. Anal. Biochem. 181:28-32.

26. Pilgram, G. S., D. C. Vissers, H. van der Meulen, S. Pavel, S. P. Lavrijsen, J. A. Bouwstra, and H. K. Koerten. 2001. Aberrant lipid organization in stratum corneum of patients with atopic dermatitis and lamellar ichthyosis. J. Invest. Dermatol. 117:710-717.
27. Bouwstra, J. A., G. S. Gooris, W. Bras, and D. T. Downing. 1995. Lipid organization in pig stratum corneum. J Lipid Res 36:685-695.
28. Pilgram, G. S., J. van der Meulen, G. S. Gooris, H. K. Koerten, and J. A. Bouwstra. 2001. The influence of two azones and sebaceous lipids on the lateral organization of lipids isolated from human stratum corneum. Biochim. Biophys. Acta 1511:244-254.
29. Moore, D. J., M. E. Rerek, and R. Mendelsohn. 1997. Lipid domains and orthorhombic phases in model stratum corneum: evidence from Fourier transform infrared spectroscopy studies. Biochem. Biophys. Res. Commun. 231:797-801.
30. Mimeault, M., and D. Bonenfant. 2002. FTIR spectroscopic analyses of the temperature and pH influences on stratum corneum lipid phase behaviors and interactions. Talanta:395–405.